The Eighteenth International Symposium on Artificial Life and Robotics 2013 (AROB 18th '13),
Daejeon Convention Center, Daejeon, Korea, January 30-February 1, 2013

Mathematical modeling of mirror based passive moiré target for orientation sensing

M.M. Hasan[1], Satoshi Tanemura[1], and Kenbu Teramoto[1]

[1] Department of Advanced Technology Fusion
Saga University, Japan
E-mail: mahbub_eeekuet@yahoo.com
(Tel: 81-80-39017956)

Abstract: Mirror based passive moiré target has been studied mathematically and numerically. Mathematical model of the passive moiré target at CCD camera sensor plate has been developed mathematical considering its orientations. Based on the mathematical model, the moiré patterns are simulated for the proposed passive target. The simulated resulted are compared to the moiré pattern produced by the existing passive moiré target. From the numerical results, it is found that the proposed passive moiré target exhibits better sensing capacities.

Keywords: Mirror-based moiré passive target, specimen grating, reflected grating, low-frequency moiré pattern.

1 INTRODUCTION

Moiré fringes based sensing technology plays an important role in shape and position control, medicare, biomechanics, liquid wave analysis and sophisticated orientation determination, due to the non-contact nature of the measurement [1-3]. The moiré technique amplifies the small changes into sensible ranges by low cost and simple arrangement. For the position and orientation sensing system, the moiré arrangement which changes its pattern according to the observer position and orientation without using light source is desirable. This type of moiré arrangement is called passive moiré. On the other hand, the moiré sensing systems require lighting arrangement to make grating pattern are called active moiré [4-5]. The research on passive moiré has been reported recently by different authors in which, a moiré target has been proposed by using two same types of specimen gratings attaching in opposite sides of a transparent substrate [6-7]. In this case, the moiré fringes become visible due to interaction of the two gratings which response to the position and orientation. The linear gratings are utilized in these reports and mathematical formulations have been developed for the arrangements. In this report, mirror based passive moiré target has been proposed in which only one specimen grating is required. In the two gratings passive moiré arrangement, two precisely identical gratings should be attached similarly in opposite sides of a substrate. But, the present mirror based one grating arrangement is free from these limitations. To the best of our knowledge, the mathematical or experimental reports on mirror based moiré fringes have not published yet. In this paper, mathematical formulations have been developed based on the orientation of the moiré target. The mathematical relations indicate the intensity of moiré fringes captured by the CCD sensor. The specimen grating function and the reflected grating functions are multiplied to form the moiré pattern. The low frequency term represents the moiré pattern.

The article is organized as follows: in section 2, the mathematical relations have been developed, in section 3, the simulated results from the mathematical relations will be shown, and at last we will draw a conclusion.

2 Mathematical Formulations

For developing mathematical formulation of the moiré fringe, the equation of 2D target plane in three dimension space has been derived. Then the equation of the line that passes through camera image plane point and focal point of the camera (projection line) are also derived. The intersection point of the target plane and projection line has been calculated. This intersection point grating intensity is the image intensity. For calculating the second grating (reflected grating) image intensity the optical ray reflection theory has been used. Then the image intensity function has been multiplied for getting moiré fringes image.

For deriving the mathematical equation consider the fig.1. First the formulations are developed based on target plane origin. Here (x, y, z) is a point on the rotated target plane. The X and Y-axis rotational angles are θ and β respectively. The relation between the rotated plane point (x, y, z) and corresponding before rotation plane point (x', y', z') can be expressed by the following equation:

$$\begin{bmatrix} x' \\ y' \\ z' \end{bmatrix} = \begin{bmatrix} \cos\beta & 0 & \sin\beta \\ \sin\beta\sin\theta & \cos\theta & -\cos\beta\sin\theta \\ -\sin\beta\cos\theta & \sin\theta & \cos\beta\cos\theta \end{bmatrix} \begin{bmatrix} x \\ y \\ z \end{bmatrix} \quad (1)$$

From the fig.1, we can write $z' = 0$ as we consider the

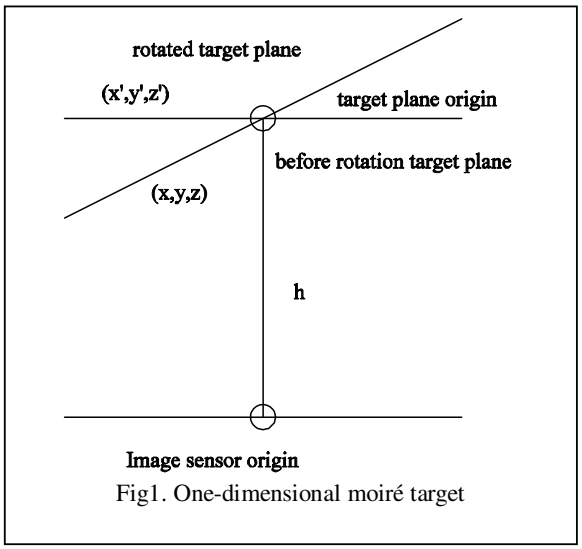

Fig1. One-dimensional moiré target

target plane canter as origin. Putting $z'=0$ in equation (1), we have:

$$z=\frac{ax-by}{c};a=\sin\beta\cos\theta;b=\sin\theta;$$
$$c=\cos\beta\cos\theta \qquad (2)$$

This is the equation of the rotated target plane considering origin at target plane centre. But if we consider origin at camera image sensor centre, then we have to modify the equation (2) by the following:

$$z=\frac{ax-by}{c}+h \qquad (3)$$

One dimensional model of camera image scanning process is shown in fig.2. In fig. 2, FOV is the field of view of the camera, f is the focal length of the camera. From fig.2, we can write the following equation:

$$f=\frac{X_{\max}}{\tan(FOV/2)} \qquad (4)$$

The straight line from target plane to image sensor plane passes through focal point $(0,0,f)$ and image sensor plane point (x_i,y_i). So, the equation of the straight line is

$$\frac{x-x_i}{-x_i}=\frac{y-y_i}{-y_i}=\frac{z}{f} \qquad (5)$$

To determine the point of rotated target plane whose intensity are scanned by the image sensor plane point (x_i,y_i), we have to find out the intersection point of equation (3) and (5). After some calculation and simplification, the coordinate of the intersection point on rotated target plane has been evaluated as following:

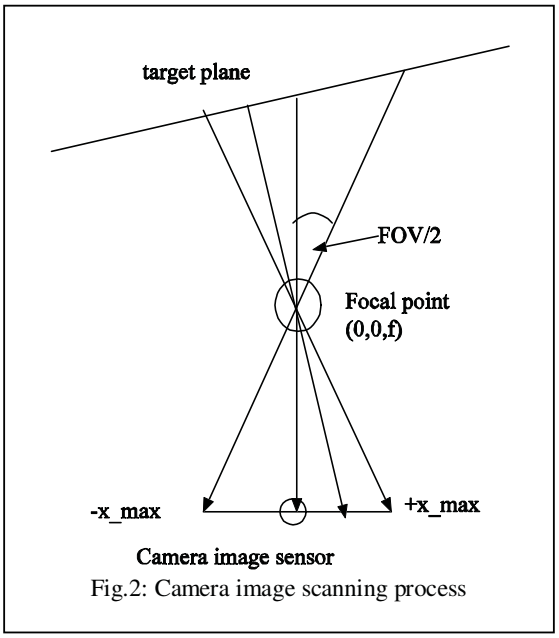

Fig.2: Camera image scanning process

$$x=\frac{cx_i(f-h)}{(cf-by_i+ax_i)}$$
$$y=\frac{cy_i(f-h)}{(cf-by_i+ax_i)} \qquad (6)$$
$$z=\frac{(ax_i-by_i)(f-h)}{(cf-by_i+ax_i)}$$

It is easier to obtain the intensity at point (x,y,z) by finding the before rotation point of point (x,y,z). If before rotation coordinate is (x',y',z'), we are interested in only x' and y'. We can write the expression of x' and y' as following:

$$x'=x\cos\beta+z\sin\beta \qquad (7)$$
$$y'=x\sin\beta\sin\theta+y\cos\theta-z\cos\beta\sin\theta$$

If the target plane grating is Fresnel zone plate (FZP), the intensity of first grating at camera image sensor plane can be expressed by equation(8)

$$G1(x_i,y_i)=\cos\left(\frac{x'^2+y'^2}{l\lambda}\right) \qquad (8)$$

The second grating is the reflected image of the attached grating (i.e. first grating). The simplified one-dimensional representation of optical ray diagram of target considering Y-axis rotation is shown in fig.3. This figure shows how grating illuminates the camera image sensor plate by reflection. So, from fig.3, it is found that image sensor point A is illuminated by the intensity of grating point B and C. Here, the target rotates around Y-axis and the rotation angle is β.In case of X-axis rotation, the situation is shown in fig.4. From fig.3 and fig.4, the Z-axis rotation will not

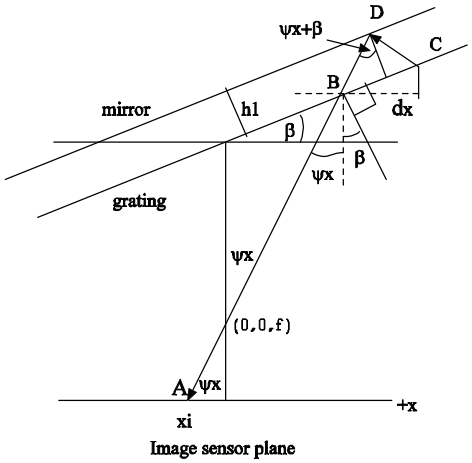

Fig.3: One-dimensional view of reflected grating considering Y-axis rotation

affect on the expression of dx and dy. So, the image sensor point (x_i, y_i) will also illuminated by the point $(x'+\mathrm{dx}, y'+\mathrm{dy})$ of the grating by reflection. If we consider $x'' = x' + dx$ and $y'' = y' + dy$, the equation of the intensity of the reflected grating can be expressed according to the equation

$$G2(x_i, y_i) = \cos\left(\frac{x''^2 + y''^2}{l\lambda}\right) \qquad (9)$$

The equation of the moiré fringes with grating can be expressed by the following equation

$$I(x_i, y_i) = G1(x_i, y_i)G2(x_i, y_i) \qquad (10)$$

we are interesting only in low frequency moiré. So, the captured moiré can be modeled by the equation

$$I(x_i, y_i) = \cos\left(\frac{2x'\mathrm{dx} + 2y'\mathrm{dy} + \mathrm{dx}^2 + dy^2}{l\lambda}\right) (11)$$

3 Simulated Results

Then numerical experiment has been performed based on the developed mathematical relations for the proposed moiré target. The simulated results for the proposed moiré target have also been compared with the two gratings moiré targets [6]. For numerical experiments, the parameters are selected considering the experimental conditions. The parameters are: field of view of the camera is 20 degree, both width and height of CCD sensor is 24mm, focal length is 30mm. From the simulated results, it is found that three closed contour moiré fringes are produced when distance from CCD to sensor target is 100mm and rotational angles are set to zero, which is shown in fig.5. Two closed contour

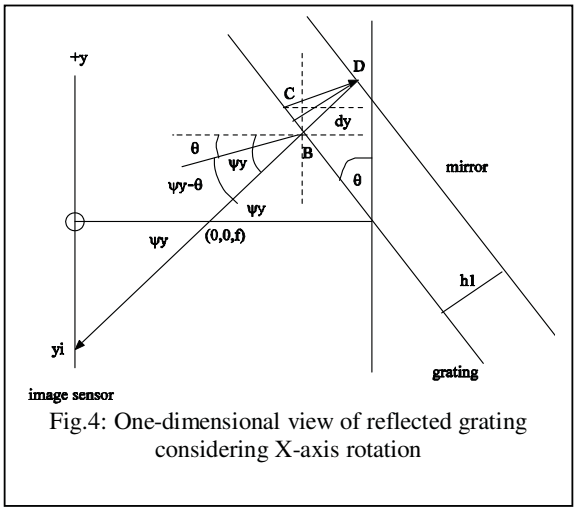

Fig.4: One-dimensional view of reflected grating considering X-axis rotation

moiré fringes are produced in this case for the two grating moiré target which is shown in fig.6. Three closed contour and one open contour moiré fringes are observed when rotation around X-axis is 2 degree $(\theta = 2\mathrm{degree})$ which is shown in fig.7. For the 2 degree angular rotation, two closed contour moiré fringes are produced for the two grating moiré target as shown in fig.8. When both X $(\theta = 2\mathrm{degree})$ and Y-axis $(\beta = 2\mathrm{degree})$ rotational angles are present, the number of contour remains same, but the moiré fringes orientation has been changes according to the ratio of θ and β as shown in fig.9. So, moiré fringes with higher number of contours are observed in our proposed moiré target. As the sensitivity depends on the numbers of contour, the proposed passive moiré target is more sensitive.

4 Conclusion

The moiré patterns produced from the proposed mirror based moiré target are compared with the moiré target described in [6]. For the same values of rotational angles, the proposed moiré target produced more contours moiré pattern, which enhances the sensing capacity and increases sensitivity.

REFERENCES

[1] E.U. Wagemann and T. Haist and M. Schönleber and H.-J. Tiziani, Fast shape and position control by Moiré-filtering and object-adapted fringe projection, Optics Communications,vol. 165, no.1-3, pp.7-10, 1999.

[2] Jinyou Shao and Yucheng Ding and Hongmiao Tian, and Xin Li and Xiangming Li and Hongzhong Liu, Digital moire fringe measurement method for alignment in imprint lithography, vol. 44, no.2, pp. 446-451, 2012.

[3] Pollyanna F. Gomes and Meinhard Sesselmann and Christina D.C.M. Faria and Priscila A. Araujo and Luci F. Teixeira-Salmela, Measurement of scapular kinematics with the moiré fringe projection technique, vol.43, no.6, pp.1215-1219,2010.

[4] Daniel Post and Bongtae Han and Peter Ifju, High Sensitivity Moire, Springer, 1994.

[5] Chia-Ming Liu and Lien-Wen Chen, Using the digital phase-shifting projection Moiré method and wavelet transformation to measure the deformation of a PMMA cantilever beam, Polymer testing,vol.24, no.5, pp. 576-582,2005.

[6] Glenn P. Tournier, Six degree of freedom estimation using monocular vision and moire patterns, M.Sc thesis, Massachusetts Institute of Technology, 2006.

[7] Eric Feron, Jim Paduano, A passive sensor for position and attitude estimation using an interferometric target, Proc. of 43rd IEEE conference on Decision and Control,vol.2,pp.1663-1669,2004.

Fig.5: Low frequency moiré fringes from proposed target when $\theta = 0, \beta = 0, h = 100mm$

Fig.6: Low frequency moiré fringes from existing target when $\theta = 0, \beta = 0, h = 100mm$

Fig.7: Low frequency moiré fringes from proposed target when $\theta = 0, \beta = 2, h = 100mm$

Fig.8: Low frequency moiré fringes from existing target when $\theta = 0, \beta = 2, h = 100mm$

Fig.9: Low frequency moiré fringes from proposed target when $\theta = 2, \beta = 2, h = 100mm$